TIMP-1 Contact Sites and Perturbations of Stromelysin 1 Mapped by NMR and a Paramagnetic Surface Probe†

S. Arumugam,‡ Christopher L. Hemme,‡ Naoki Yoshida,§ Ko Suzuki,§ Hideaki Nagase,§ Mark Berjanskii,‡ Bin Wu,‡ and Steven R. Van Doren*,‡

Department of Biochemistry, 117 Schweitzer Hall, University of Missouri, Columbia, Missouri 65211, Department of Biochemistry and Molecular Biology, 3901 Rainbow Boulevard, University of Kansas Medical Center, Kansas City, Kansas 66160-7421

Received January 20, 1998; Revised Manuscript Received April 16, 1998

ABSTRACT: Surfaces of the 173 residue catalytic domain of human matrix metalloproteinase 3 (MMP-3(ΔC)) affected by binding of the N-terminal, 126 residue inhibitory domain of human TIMP-1 (N-TIMP-1) have been investigated using an amide-directed, NMR-based approach. The interface was mapped by a novel method that compares amide proton line broadening by paramagnetic Gd−EDTA in the presence and absence of the binding partner. The results are consistent with the X-ray model of the complex of MMP-3(ΔC) with TIMP-1 (Gomis-Rüth et al. (1997) *Nature 389,* 77−81). Residues Tyr155, Asn162, Val163, Leu164, His166, Ala167, Ala169, and Phe210 of MMP-3(ΔC) are protected from broadening by the Gd−EDTA probe by binding to N-TIMP-1. N-TIMP-1-induced exposure of backbone amides of Asp238, Asn240, Gly241, and Ser244 of helix C of MMP-3(ΔC) to Gd−EDTA confirms that the displacement of the N-terminus of MMP-3(ΔC) occurs not only in the crystal but also in solution. These results validate comparative paramagnetic surface probing as a means of mapping protein−protein interfaces. Novel N-TIMP-1-dependent changes in hydrogen bonding near the active site of MMP-3(ΔC) are reported. N-TIMP-1 binding causes the amide of Tyr223 of MMP-3(ΔC) bound by N-TIMP-1 to exchange with water rapidly, implying a lack of the hydrogen bond observed in the crystal structure. The backbone amide proton of Asn162 becomes protected from rapid exchange upon forming a complex with N-TIMP-1 and could form a hydrogen bond to N-TIMP-1. N-TIMP-1 binding dramatically increases the rate of amide hydrogen exchange of Asp177 of the fifth β strand of MMP-3(ΔC), disrupting its otherwise stable hydrogen bond.

Matrix metalloproteinase 3 (MMP-3),[1] or stromelysin 1, is a member of a family of zinc- and calcium-dependent proteases which degrade components of the extracellular matrix during processes of reproduction, development, wound repair, arthritis, atherosclerosis, and cancer (*1*−*4*). Tissue inhibitors of metalloproteinases (TIMPs) regulate the activity of MMPs by forming 1:1 noncovalent complexes with subnanomolar dissociation constants (*5*).

Recent crystallographic studies have shown that wedge-shaped TIMP-1 interacts with the active site of the catalytic domain of stromelysin 1 (MMP-3(ΔC)). The 126 residue, N-terminal fragment of TIMP-1 (N-TIMP-1), with residues 127−184 deleted, folds independently (*6*, *7*) and retains greater than 90% of the free energy of association with MMPs. Because N-TIMP-1 contains only three disulfides, it is much more easily refolded from *Escherichia coli* inclusion bodies than is full-length TIMP-1 which contains six disulfides (*8*). Because the affinity of N-TIMP-1 for MMPs -1, -2, and -3 is only 6−8-fold less than the affinity of recombinant full-length TIMP-1, N-TIMP-1 is expected to bind MMPs in a manner similar to full-length TIMP-1. Thus, N-TIMP-1 is well-suited for structural studies of its complex with an MMP catalytic domain in solution by NMR. Likewise, N-TIMP-2, having 45% sequence identity with N-TIMP-1, has been amenable to structure determination (*9*) and to chemical shift mapping of its MMP-3(ΔC) recognition surface (*10*).

Mapping of the surface of human MMP-3(ΔC) recognized by the N-terminal domain of human TIMP-1 (N-TIMP-1) in nearly physiological salt solution is reported herein, on the basis of three backbone-directed assays using NMR spectroscopy. Changes in chemical shift of amide groups (*11, 12*), protection of amide protons from hydrogen exchange with solvent (*13*) on a subsecond time scale, and protection of amide protons from line broadening by a paramagnetic probe of gadolinium-EDTA permit delineation of the interaction surface of the 33 kDa complex of the MMP-3 catalytic domain with N-TIMP-1.

† This work was supported by an Arthritis Foundation Arthritis Investigator award to S.R.V. and NIH Grants AR39189 and AR40944 to H.N. The Bruker DRX-500 instrument used was purchased in part with funding from NSF Grant 8908304.

* Corresponding author. Phone: 573-882-5113. Fax: 573-884-4812. E-mail: vandoren@ixta.biochem.missouri.edu.

‡ University of Missouri.

§ University of Kansas Medical Center.

[1] Abbreviations: DTT, dithiothreitol; HSQC, heteronuclear single quantum coherence; IPTG, isopropylthiogalactoside; MMP, matrix metalloproteinase; MMP-3(ΔC), catalytic domain of stromelysin 1 lacking the C-terminal domain; N-TIMP-1, amino-terminal domain of tissue inhibitor of metalloproteinases 1; TEMPO, 2,2,6,6-tetramethylpiperidine-*N*-oxyl; TIMP, tissue inhibitor of metalloproteinases.

S0006-2960(98)00128-7 CCC: $15.00
Published on Web 06/18/1998

The mapping of a protein−protein interface using protection from the line broadening induced by a soluble paramagnetic probe of the surface is a novel extension of the method of paramagnetic surface probing. Exclusion of the probe from the interface clarifies which regions truly become buried upon binding. The paramagnetic NMR line broadening agents hydroxy-TEMPO and chelated gadolinium(III) have been employed to monitor surface exposure of lysozyme and of ubiquitin (*14*, *15*). Aliphatic proton T_1 values, being sensitive to paramagnetic relaxation sinks, have been used to monitor surface exposure in drug−enzyme complexes (*16*). Comparison of paramagnetic broadening effects upon HSQC spectra of an isotopically enriched protein in the presence and absence of a binding partner provides a convenient and meaningful assay of the intermolecular interface.

The consistency of the N-TIMP-1-binding surface of MMP-3(ΔC), inferred from amide chemical shift perturbation and paramagnetic surface probing, with the crystallographic TIMP-1−MMP-3(ΔC) interface validates comparative paramagnetic probing as an excellent means of quickly mapping protein−protein interfaces in solution by NMR.

MATERIALS AND METHODS

Isotopic Enrichment of Cultures Expressing MMP-3(ΔC). *E. coli* BL21(DE3) transformed with human MMP-3(ΔC) cDNA in pET3a (the generous gift of Prof. Keith Brew of the University of Miami) was grown in M9 minimal media at 37 °C containing 50 mg/L ampicillin (Sigma, St. Louis, MO). ^{15}N-labeled MMP-3(ΔC) was prepared by adding 1g/L $^{15}NH_4Cl$ (99% ^{15}N) to the M9 medium instead of unlabeled ammonium chloride. ^{13}C- and ^{15}N-labeled MMP-3 samples were prepared using either M9 media containing 1g/L $^{15}NH_4Cl$ and 0.25% ^{13}C-labeled glucose (99% ^{13}C) (Isotec, Miamisburg, OH) or M9 media containing 1g/L $^{15}NH_4Cl$ and 0.20% ^{13}C-labeled glucose supplemented with 1.6% (v/v) of a 10x concentrate of ^{13}C/^{15}N-labeled Celtone-CN (Martek Biosciences Company, Columbia, MD). To induce the production of recombinant MMP-3(ΔC), IPTG (Calbiochem, La Jolla, CA) was added to the bacterial cultures to a final concentration of 0.4 mM when the cell density reached an optical density at 600 nm of 0.6−0.8. MMP-3(ΔC) specifically labeled with ^{15}N at leucine or tyrosine residues was prepared in M9 media supplemented with all amino acids at 0.1g/L except the leucine or tyrosine, with 1 g/L each of adenine, guanosine, and uracil and 0.4 g/L of thymine and cytosine (*17*, *18*). ^{15}N-labeled L-leucine (^{15}N > 98%) (Cambridge Isotope Laboratories, Inc., Andover, MA) was added to 0.06g/L upon inoculation. ^{15}N-labeled L-tyrosine (^{15}N 95-99%) (Cambridge Isotope Laboratories, Inc., Andover, MA) was added to 0.06 g/L upon induction with IPTG.

Preparation of MMP-3(ΔC). ^{15}N-enriched MMP-3(ΔC) was refolded from inclusion bodies and purified as described (*19*). Active ^{13}C- and ^{15}N-enriched MMP-3(ΔC) was purified from the soluble fraction of the *E. coli* expression system using a simplification of the method described by ref *20*. Lysed cells were spun at 14 000 rpm for 30 minutes at 4 °C. The pellet was discarded and the supernatant was further spun at greater than 100000*g* using an ultracentrifuge at 4 °C for at least 12 h. Supernatant was collected and loaded onto a Q-Sepharose column equilibrated with 20 mM Tris-HCl, 5 mM $CaCl_2$, and 0.02% NaN_3 at pH 8.0 at 4 °C. The protein was eluted with a linear gradient of 0-0.3 M NaCl in the equilibration buffer. Pure pro-MMP-3(ΔC) was pooled, activated, and further purified as described previously (*20*).

Preparation of 1:1 Complexes of Isotopically Enriched, Active MMP-3(ΔC) with Unlabeled N-TIMP-1. The N-terminal inhibitory domain of TIMP-1 was prepared as reported (*8*). Complexes of ^{15}N- or ^{13}C/^{15}N-labeled active MMP-3(ΔC) 1:1 with unlabeled N-TIMP-1 were prepared on the basis of an activity assay of MMP-3 using a fluorogenic synthetic substrate (*21*). A slight excess of N-TIMP was used to ensure that all of the MMP-3(ΔC) is in complex with N-TIMP-1.

NMR Sample Preparation. Buffers for the purified MMP-3 and the complex were exchanged with a buffer containing 100 mM NaCl, 15 mM $CaCl_2$, 3 μM $ZnCl_2$, 1 mM NaN_3, 7% D_2O, and 20 mM perdeuterated Tris (Isotec, Miamisburg, OH), pH 7.2 when measured at 24 °C. The protein concentrations were kept below 0.8 mM (*22*). Eight millimeter Shigemi microcells (Shigemi Standard & Joint Co. Ltd, Tokyo, Japan) were used with about 650 μL of sample for NMR.

NMR Spectroscopy. The NMR experiments were carried out using a Bruker DRX-500 NMR spectrometer fitted in general with a Nalorac 8 mm probe with shielded z-gradient and triply tuned to ^{15}N, ^{13}C, and ^{1}H (Nalorac Corporation, Martinez, CA). Most HSQC-type spectra employed the "fast HSQC" method to minimize saturation of the water resonance (*23*). Low-power GARP decoupling sequence was used to decouple ^{15}N during acquisition (*24*). SYBYL TRIAD version 6.2 or 6.3 (Tripos Inc., St. Louis, MO) was used for processing and interpreting NMR spectra. ^{15}N and ^{13}C chemical shifts were referenced with respect to ammonium nitrate and 2,2-dimethyl-2-silapentane-5-sulfonate, respectively. States-TPPI quadrature detection (*25*) was used in all of the indirect dimensions.

Spectra Collected for Reassignment of Backbone Amide Resonances. Triple resonance 3D experiments like CT-HNCA (*26*), (HA)CA(CO)NH, and HA(CACO)NH spectra (*27*, *28*) were collected for MMP-3(ΔC) of 19.5 kDa. 3D CT-HNCA and CT-HN(CO)CA (*26*) spectra were collected for N-TIMP-1-inhibited MMP-3(ΔC) of 33 kDa. These spectra enabled the reassignment of the backbone amide resonances of free MMP-3(ΔC) and the assignment of those resonances when in complex with N-TIMP-1. All triple resonance spectra were enhanced using pulsed field gradients (*29*) and WATERGATE with a 3-9-19 composite pulse (*30*). Triple resonance spectra were mirror-image linear predicted (*31*) in the ^{15}N dimension of each and were linear predicted in the ^{13}C dimension of each, to improve resolution.

^{15}N-separated NOESY-HSQC spectra (*32*) were acquired with the enhancement of the fast HSQC method to minimize water saturation (*23*). NOESY mixing times were 90 ms for free MMP-3(ΔC) and 55 and 80 ms in spectra of its complex with unlabeled N-TIMP-1.

Quantitation of N-TIMP-1 Amide Shift Changes. The size of each N-TIMP-1-induced change in amide peak position of the MMP-3(ΔC) spectra is quantified as the Pythagorean relation:

$$\Delta NH = (\Delta H^2 + (\Delta N/6)^2)^{1/2} \quad (1)$$

where ΔH and ΔN are chemical shift changes in parts per million along the proton and nitrogen axes for a particular amide. The factor of about six scales the nitrogen shift changes down for equal weighting with proton shift changes. Similar quantitation has been reported (*33*).

Protection from Line Broadening by Gd−EDTA Paramagnetic Probe. The novel extension of lanthanide-induced relaxation to mapping of a protein−protein recognition surface is straightforward. While proton T_1 and T_2 values are quite sensitive to paramagnetic relaxation, fitting of amide proton relaxation is complicated by cross relaxation and chemical exchange with water. Consequently, the line-broadening effects of Gd−EDTA upon active and N-TIMP-1-inhibited MMP-3(ΔC) are herein compared as a simple difference in normalized height of amide HSQC peaks. 2D ^{1}H-^{15}N fast HSQC experiments were carried out for both free MMP-3(ΔC) and MMP-3(ΔC) bound by N-TIMP-1 in the presence of 0.0, 1.0, 2.0, and 3.0 mM concentrations of paramagnetic Gd−EDTA complex. Gd(III), having a long electron spin relaxation time, is a paramagnetic relaxation agent, rather than a shift reagent. Line broadening was measured as a ratio of the height of a backbone amide resonance at a given concentration of Gd−EDTA to the height when no paramagnetic probe is present. The error in the calculated broadening may be higher for overlapping peaks.

For $\omega\tau_C$ values typical of protein NMR, the Solomon−Bloembergen description of paramagnetic line broadening simplifies to $T_2^{-1} \propto \gamma_H^2 S(S+1) r^{-6} \tau_C$, where $\tau_C^{-1} = \tau_R^{-1} + \tau_e^{-1}$. Gd(III), having electron spin S of $^7/_2$, is a much stronger broadening agent than spin $^1/_2$ agents such as TEMPO. The correlation time τ_C is dominated by the rotational correlation time τ_R because the electron spin relaxation time τ_e of Gd(III) at high field is much longer than τ_R. Since the proton line broadening by Gd(III) is proportional to τ_R (*34*), a lower concentration of Gd−EDTA was needed to broaden the proton lines in the N-TIMP-1−MMP-3(ΔC) complex to a similar extent as in free MMP-3(ΔC). The broadening of free MMP-3(ΔC) amide protons by 3 mM Gd−EDTA was found to give an overall broadening of amide protons similar to the more slowly tumbling N-TIMP-1−MMP-3(ΔC) complex by 2 mM Gd−EDTA. Consequently, relative heights of amide peaks of free MMP-3(ΔC) broadened by 3 mM Gd−EDTA were subtracted from the relative heights of peaks of MMP-3(ΔC), bound to N-TIMP-1 and broadened by 2 mM Gd−EDTA.

Measurement of Hydrogen Exchange Rates on the Sub-Second Time Scale. A pulse sequence to monitor the exchangeable protons, WEXII-FHSQC (*35*), has been used to measure the proton exchange rates of MMP-3(ΔC) when it was free and in a 1:1 complex with N-TIMP-1. This pulse sequence suppresses NOE contributions to the amide resonance. Mixing times during which the exchange between water protons and the amide protons occur ranged typically from 12.5 to 87.5 ms at 12.5 ms intervals.

Selective T_1 values of amide protons were measured using an inversion-recovery approach (*36*) by selectively inverting the amide protons with an I-BURP-2 pulse (*37*) and waiting for variable lengths of time before applying the fast HSQC pulse sequence (*23*). To avoid bias from hydrogen exchange with water, average amide proton T_1 values were determined from a few dozen well-resolved peaks for which the hydrogen exchange rates are less than one per second. This "selective" T_1 measurement retains contributions from cross relaxation with other amide and aromatic protons, likely to be relatively small. Supposing systematic error of 1.5-fold in T_1 can be present, fitted hydrogen exchange rates are perturbed by less than 20% for the free MMP-3(ΔC) and by less than 30% for the N-TIMP-1-inhibited MMP-3(ΔC). The water proton T_1 was measured using a simple inversion-recovery sequence with a very weak pulsed field gradient present to prevent radiation damping during the entire delay between the inversion pulse and the read pulse.

The relative growth of magnetization of exchangeable protons was fitted to an equation describing such an exchange phenomenon (*38*) which can be derived from generalized expressions for exchange spectroscopy (*39*), in this case without contributions from NOE.

$$I/I_0 = k_{NH}/(R_{1NH} + k_{NH} - R_{1water}) \times \{\exp(-R_{1water}T_m) - \exp[-(R_{1NH} + k_{NH})T_m]\} \quad (2)$$

where I is the height of a particular peak at a mixing time T_m. I_0 is the height of that particular peak obtained under the same conditions as the exchange experiment except that spin echo delays and any mixing period are absent. R_{1NH} and R_{1water} are the spin-lattice relaxation rates of the amide proton and that of the solvent water, respectively. These rates were measured for the free MMP-3 and MMP-3 in complex with N-TIMP-1 separately as described above. The amide proton exchange rate k_{NH} has been obtained for the exchanging amide protons by fitting the height ratios as a function of the mixing time with a nonlinear least-squares fitting procedure. Average R_{1NH} values of 7.5/s and 13.9/s were obtained from the selective NH T_1 measurements, for the free MMP-3 and the complex respectively, and were used in the fits. The hydrogen exchange protection factor in the context of protein−protein interactions is defined as k_{free}/k_{bound} (*13*), where k_{free} is the hydrogen exchange rate measured for uninhibited MMP-3(ΔC) and k_{bound} is the rate measured for MMP-3(ΔC) inhibited by N-TIMP-1.

RESULTS

Sample Stability. The NMR spectra of MMP-3(ΔC) refolded from the insoluble fraction are identical to those from the soluble fraction. MMP-3(ΔC) in 1:1 complex with N-TIMP-1 is very stable at near neutral pH, and its amide HSQC spectra are homogeneous. At concentrations of 0.5−1 mM, the complex is soluble at temperatures up to 37 °C.

Resonance Assignments. Assignments of the amide peaks of free MMP-3(ΔC) enabled comparison of "footprinting" results with MMP-3(ΔC) bound by N-TIMP-1. HNCA, (HA)CA(CO)NH, HA(CACO)NH, and ^{15}N-separated NOESY spectra were employed to assign the NMR peaks of backbone amides of free MMP-3(ΔC). Specific ^{15}N-enrichment in leucine or tyrosine residues confirmed residue-type identification. For free MMP-3(ΔC), 92% of the 158 non-proline residues are unambiguously assigned.

The high affinity of MMP-3(ΔC) for N-TIMP-1, having a K_I of 1.9 nM (*8*) and a k_{on} of about 10^6 M^{-1} s^{-1} (*5*), implies an exceedingly slow dissociation rate for the complex. Since $k_{off} \ll \Delta\nu$, where $\Delta\nu$ is a small difference in chemical shift between free MMP-3(ΔC) and MMP-3(ΔC) inhibited by

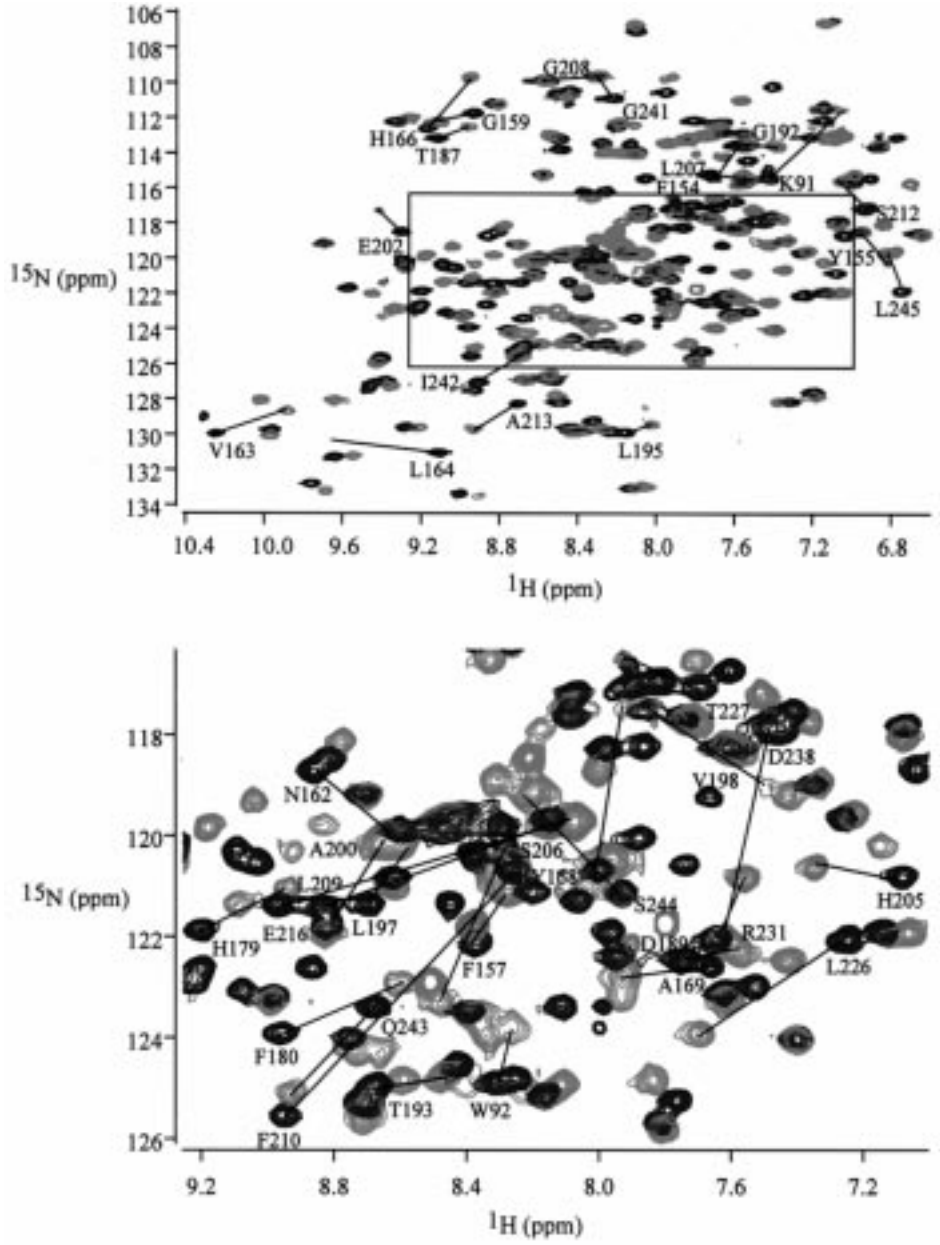

FIGURE 1: ^{1}H-^{15}N HSQC spectra of human MMP-3(ΔC), uninhibited (blue contours) and inhibited by human N-TIMP-1 present at 1:1 stoichiometry (red contours). The peaks experiencing the largest shifts, above the threshold in Figure 2A, are labeled. The lower panel is an expansion of the boxed region.

N-TIMP-1, reassignment of amide resonances of the complex demanded a similar set of 3D assignment spectra plus HN-(CO)CA and HNCO spectra, rather than titration of HSQC spectra. For MMP-3(ΔC) in complex with N-TIMP-1, 89% of the 158 non-proline residues are unambiguously assigned.

Changes in Amide Spectra of MMP-3(ΔC) Induced by N-TIMP-1. Changes in backbone amide shifts for MMP-3(ΔC) upon binding N-TIMP-1 are significant for a third of the residues (Figures 1 and 2A). Perturbed residues Phe154, Tyr155, and Phe157 occur in the loop connecting strands III and IV in the vicinity of the structural zinc above the beta sheet (Figures 2A and 3). Closer to the active site, large shift perturbations occur for residues Asn162 through Ala169, which includes strand IV. Significant amide shifts are also found among residues toward the end of the loop connecting strand V and helix B, that is, Thr187, Asp189, Gly192, and Thr193. Helix B residues Leu195 through Ser206 exhibit marked N-TIMP-1-induced shifts (Figures 2A and 3). Other residues with notable shifts include Leu207-Phe210, Ser212, Ala213, Glu216, Leu222, Tyr223, Ser225-Thr227, and Arg231 in the loop connecting helix B to helix C which skirts the active site. Surprisingly, amide shifts also occur for residues distant from the active site, including residues Asp238 and Gly241-Leu245 in the C helix, residues Thr85, Ile89 and Lys91-Arg93 near the N-terminus, and residues His179 and Phe180 of β strand V. To help recognize chemical shift changes occurring for residues outside the direct N-TIMP-1 recognition surface, two surface protection studies were conducted.

Protection from Gd−EDTA, Paramagnetic Surface Probe. Relative amide peak heights were estimated as a ratio of the height of a particular peak in the ^{1}H-^{15}N HSQC with paramagnetic probe present to the height with no paramagnetic probe present. Relative heights for free MMP-3(ΔC) with 3 mM Gd−EDTA present are subtracted from relative heights for MMP-3(ΔC) bound to N-TIMP-1 with 2 mM

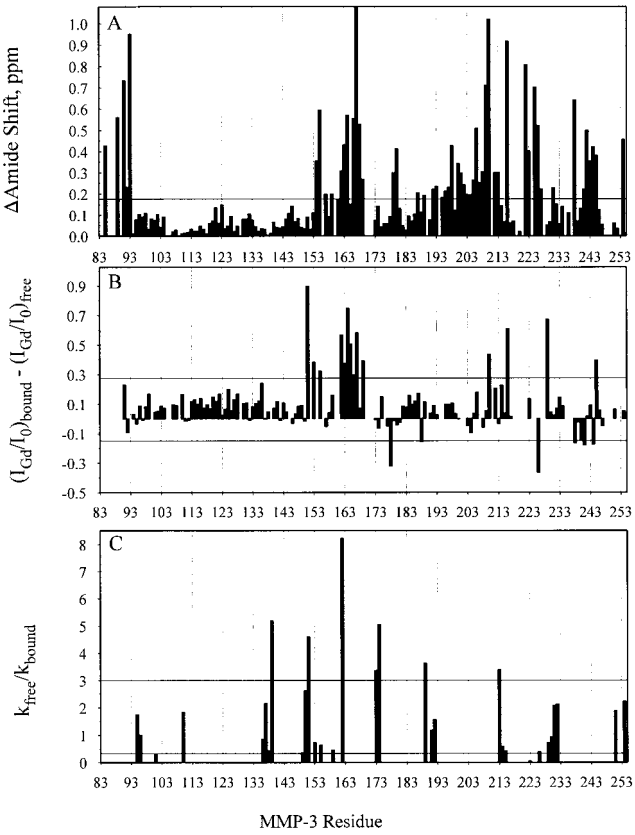

FIGURE 2: (A) Plot of N-TIMP-1-induced changes in chemical shifts of MMP-3(ΔC) amide peaks, using eq 1. (B) N-TIMP-1 protection and exposure of MMP-3(ΔC) amides to line broadening by Gd−EDTA. Normalized heights of amide peaks of free MMP-3(ΔC), $(I_{Gd}/I_0)_{free}$, with 3 mM Gd−EDTA added were subtracted from normalized heights of amide peaks of N-TIMP-1-inhibited MMP-3(ΔC), $(I_{Gd}/I_0)_{bound}$, with 2 mM Gd−EDTA added. Reference heights, I_0, of the peaks from the spectra obtained before the addition of the Gd−EDTA were used to normalize heights at a given concentration of the paramagnetic probe. Positive values above the upper threshold indicate protection from the broadening effects in the complex, whereas negative values below the lower threshold indicate increased Gd−EDTA probe accessibility. (C) The ratio of the exchange rate of an amide proton when the MMP-3(ΔC) is uninhibited, k_{free}, to the exchange rate when the MMP-3(ΔC) is bound to N-TIMP-1, k_{bound}. Those residues having a ratio much less than 1.0 can be better appraised in Table 1. Residues that are not assigned in spectra when MMP-3(ΔC) is either free or bound to N-TIMP-1, residues whose amides fail to undergo hydrogen exchange with water ≥1.4 times/s, and all proline residues are given a value of 0.0 in all three plots.

Gd−EDTA present (Figure 2B). The complex, having a longer rotational correlation time roughly in proportion to the larger mass, is proportionately more sensitive to the paramagnetic probe (*34*); thus a lower probe concentration was used with the complex for comparison with the free protease.

Amide proton resonances of residues His151, Asp153, and Tyr155, of the S-shaped, metal-binding loop joining strands III and IV, are significantly protected from broadening when in the MMP-3(ΔC)−N-TIMP-1 complex (Figures 2B and 4). The amide protons of Asn162-Ala167 and Ala169 near the active site are very well protected from the broadening effects of Gd−EDTA. Amide protons of residues Phe210, Glu216, and Leu229 that are in the loop connecting helices B and C are also protected from the Gd−EDTA broadening. Ser212 and Asn214 are protected to a lesser extent (Figure 2B). Leu245, more distant from the active site, experiences

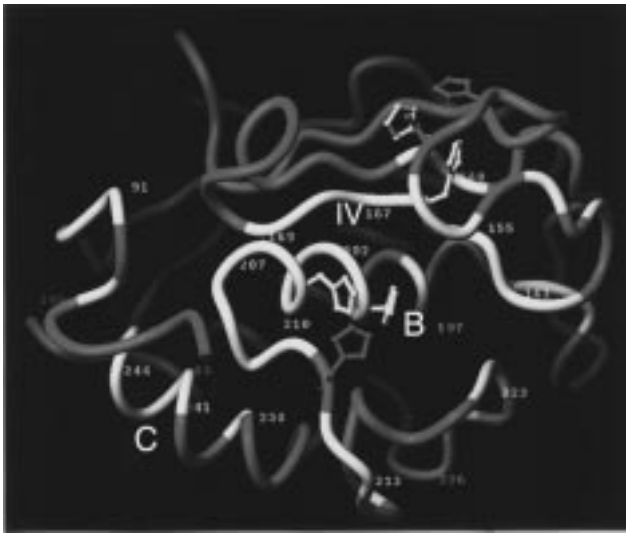

FIGURE 3: Changes in amide chemical shifts in MMP-3(ΔC) induced by N-TIMP-1 binding plotted on an α carbon trace of the minimized, average solution structure of MMP-3(ΔC) (*43*), using MOLMOL (*44*). Residues experiencing changes higher than the threshold in Figure 2A are colored yellow. Side chains which coordinate zinc are drawn. Beta strand IV, helix B, and helix C are labeled.

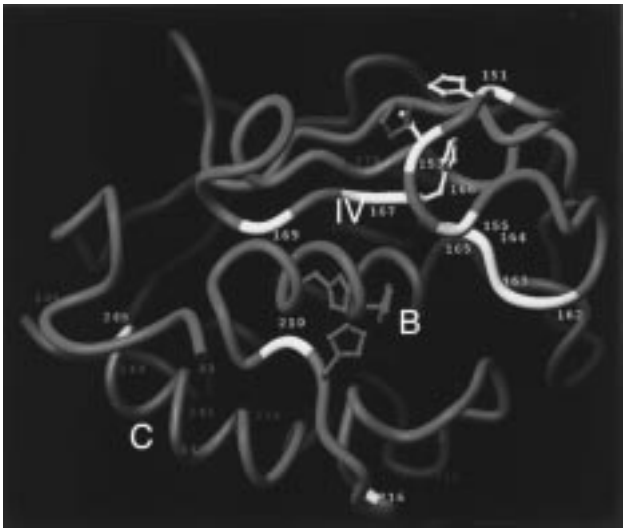

FIGURE 4: Changes in amide line broadening by the paramagnetic probe Gd−EDTA, comparing broadening in the presence and absence of N-TIMP-1, plotted upon the minimized, average solution structure of MMP-3(ΔC). Residues experiencing protection of the amide from probe in the presence of N-TIMP-1 above the upper threshold of Figure 2B are colored yellow. Residues with increased exposure to the probe in the presence of N-TIMP-1 (downward deflections below the threshold in Figure 2B) are colored red.

some protection from the probe in the presence of N-TIMP-1. Interestingly, amide protons of Ala178, Lys188, Leu226, Asp238, Asn240, Gly241, and Ser244 are significantly more *exposed* to the broadening effects of the paramagnetic probe when MMP-3(ΔC) is bound by N-TIMP-1.

Changes in Sub-Second Amide Proton Exchange Rates of MMP-3(ΔC)*, Induced by N-TIMP-1 Binding.* The ratio of the faster amide hydrogen exchange rates of the free MMP-3(ΔC) to those of the N-TIMP-1-inhibited form are plotted in Figure 2C. An exchange rate of less than 1.4/s is assumed for comparison wherever an exchange peak is not observed. The most rapid of exchange rates, greater than 40/s, measurable by this HSQC-resolved approach have an

increased uncertainty because the rates are large relative to the $^1J_{HN}$ of 92 Hz used by the INEPT steps, weakening the peaks in the reference spectrum. Upon consideration of the error in measuring and fitting the rates of exchange, a value of k_{free}/k_{bound} of 3.0 or more is deemed an experimentally significant protection of the amide from hydrogen exchange, caused by N-TIMP-1 binding to MMP-3(ΔC). Likewise, a value of 0.33 or less for k_{free}/k_{bound} is considered a significant exposure of the amide in MMP-3(ΔC) to greater hydrogen exchange upon binding to N-TIMP-1. Amide protons of Glu139, His151, Asn162, Gly173, Ile174, Asp189, and Ala213 of MMP-3(ΔC) show measurable protection from hydrogen exchange upon binding N-TIMP-1. Of these eight sites, the amides of Asn162 and possibly Ala213 are proposed to lie on the N-TIMP-1 recognition surface. The slowing of amide hydrogen exchange rates for Glu139, Glu150, His151, Gly173, Ile174, and Asp189 and the increase in rates for Ile101, Arg149, Asp177, Tyr223, Leu226, and Ser244 of MMP-3(ΔC) upon the inhibitory binding of N-TIMP-1 might suggest subtle conformational adjustments outside the binding interface.

DISCUSSION

Consistency between Protection from Paramagnetic Probe and X-ray Model. Protection from line broadening by Gd−EDTA probe, supplemented by changes in amide chemical shifts, enables inferences about the contacts between N-TIMP-1 and MMP-3(ΔC) which agree remarkably well with the contacts reported for the crystal structure of the TIMP-1−MMP-3(ΔC) complex. N-TIMP-1 binding protects amide protons of MMP-3(ΔC) residues Tyr155, Asn162, Val163, Leu164, His166, Ala167, Ala169, and Phe210 from broadening by the paramagnetic probe. These residues lie in the interface between MMP-3(ΔC) and TIMP-1, as demonstrated by the crystal structure (*40*) (Figure 2B and 4).

Displacement of N-terminus of MMP-3(ΔC) from its C Helix upon TIMP-1 Binding Confirmed in Solution. Protection from the broadening of proton NMR peaks by the chelated gadolinium relaxation sink is a straightforward way to distinguish burial in the protein−protein interface from binding-induced exposure outside this interface. Illustrating this is the increased exposure of backbone amides of Asp238, Asn240, Gly241, and Ser244 of helix C of MMP-3(ΔC) upon binding to N-TIMP-1. The amide chemical shift perturbations (Figures 2A and 3) alone are not enough to suggest such exposure. Exposure of helix C in solution is quite consistent with the crystallographic observation that TIMP-1 binding causes the F83 α-ammonium group of MMP-3(ΔC) to move a dramatic 15 Å away from its position otherwise salt-bridged to Asp237 (*40*). The consistency of protections in the interface and of exposure of helix C with the X-ray model validate the use of comparative paramagnetic probing of protein−protein interfaces with chelated gadolinium.

Limitations of Comparative Paramagnetic Broadening of Amides in Probing Protein−Protein Interfaces. Conformational changes linked to binding which increase exposure to paramagnetic probe, for example, the N-TIMP-1-induced exposure of helix C of MMP-3(ΔC), may be easily recognized. However, binding-linked conformational changes outside the interface which increase protection from paramagnetic probe can be confused with protection within the interface.

Residues just inside or just outside the protein−protein interface may experience moderate protection from broadening by paramagnetic solution probe. Defining the edge of the interface using paramagnetic protection may thus be imprecise. The amides of MMP-3(ΔC) residues Ser212 and Asn214 experience modest degrees of N-TIMP-1-dependent protection from Gd−EDTA (Figures 2B and 4). The modest slowing of the hydrogen exchange of Ala213 upon binding of N-TIMP-1 is consistent with the modest protection of its neighbors from broadening by Gd−EDTA. To what extent Ser212, Ala213, and Asn214 lie just inside or outside the interface is not fully clear either from paramagnetic probing or from the published backbone structure of the X-ray model (*40*). The modest protections are near the background "noise" in Figure 2B. Much of this "noise" may arise from systematic local variations in the surface topography, polarity, and electrostatic field of MMP-3(ΔC), free or inhibited. Furthermore, paramagnetic probe concentrations chosen imperfectly to compensate for the difference in rotational correlation times between free and bound protein will cause an overall shift up or down of the data plotted in the style of Figure 2B.

The backbone amides of helix B of MMP-3(ΔC) are notably less sensitive to protection from broadening by Gd−EDTA probe. The side chains of His201, His205, and presumably Val198 of MMP-3(ΔC) make contacts with TIMP-1 in the crystallographic model (*40*). The lower sensitivity of the backbone of helix B to broadening by the paramagnetic probe (see Supporting Information) can be explained by the deep burial of the backbone of helix B. The presence or absence of N-TIMP-1 binding thus has a limited effect on broadening of amides of helix B. Though the paramagnetic protection assay says little about the participation of the backbone of helix B in binding, nearly all of the backbone amides of buried helix B of MMP-3(ΔC) experience sizable changes in chemical shift upon binding of N-TIMP-1 (Figure 2A and 3), reflecting their proximity to the interface.

Since only backbone amides were monitored for convenience, inferences about contacts involving side chains are more tenuous. For residues Val198, His201, and His205 of helix B (whose side chains make contacts with TIMP-1 (*40*)), the backbone seems to be sufficiently far from these contacts that the amides do not experience enough N-TIMP-1-dependent protection from broadening by Gd−EDTA to reveal side chain contacts with N-TIMP-1. Among MMP-3(ΔC) residues Tyr155, Asn162, Val163, Leu164, His166, Ala167, Ala169, and Phe210 implicated by both crystallography and the paramagnetic protection assay to lie in TIMP-binding interface, some of the contacts appear to involve hydrophobic side chains. Yet the backbone amides are still protected from the Gd−EDTA probe and suggest interactions.

A Subtle and Novel Adjustment in MMP-3(ΔC) on Binding N-TIMP-1, Outside the Interface. N-TIMP-1-induced exposure of the amide of Ala178 to Gd−EDTA may be correlated with N-TIMP-1-induced release of the neighboring Asp177 amide from slow to rapid exchange with water (Table 1 and Figure 2C). The amide of Asp177 in MMP-3(ΔC) bound to a small synthetic inhibitor forms a hydrogen bond with the carbonyl oxygen of Ile174 (*41, 42*). The putative disruption of this Asp177 to Ile174 hydrogen bond

Table 1: Comparison of Hydrogen Exchange Rates of MMP-3(ΔC) in the Absence and Presence of N-TIMP-1 (at 1:1.1 ratio), Observed on a Millisecond Scale[a]

residue	k, s^{-1} of free MMP-3(ΔC)	k, s^{-1} of MMP-3(ΔC) inhibited by N-TIMP-1	k_{free}/k_{bound}[b]
Thr95	21.8	12.5	1.7
His96	<1.4[c]	1.4	<1.0[c]
Ile101	<1.4[c]	4.6	<0.3[c]
Lys110	4.2	2.3	1.8
Tyr136	3.2	3.8	0.8
Glu137	6.5	3.0	2.2
Gly138	2.6	6.1	0.4
Glu139	7.3	<1.4[c]	>5.2[c]
Arg149	3.1	9.0	0.3
Glu150	8.1	3.1	2.6
His151	6.4	<1.4[c]	>4.6[c]
Asp153	6.9	9.6	0.7
Tyr155	1.8	2.9	0.6
Gly159	4.9	10.8	0.5
Asn162	11.5	<1.4[c]	>8.2[c]
Gly173	22.5	6.7	3.4
Ile174	48.2	9.6	5.0
Asp177	<1.4 (<1/h)	24.8	<0.00001[d]
Asp183	<1.4 (<1/h)	2.3	<0.0001[d]
Asp189	8.5	2.4	3.5
Thr191	12.0	10.2	1.2
Gly192	2.8	1.8	1.6
Ala213	46.5	13.8	3.4
Asn214	2.7	4.7	0.6
Thr215	<1.4[c]	2.5	<0.6[c]
Tyr223	<1.4[c]	28.2	<0.05[c]
Leu226	<1.4[c]	3.7	<0.4[c]
Leu229	17.5	24.5	0.7
Thr230	12.4	13.4	0.9
Arg231	4.0	1.9	2.1
Phe232	7.3	3.4	2.1
Ser244	<1.4[c]	4.6	<0.3[c]
Asp251	15.6	8.2	1.9
Glu254	19.3	8.7	2.2

[a] The uncertainty in the fitting of rates is at most about 20% for free MMP-3 and at most about 30% for the complex when varying backbone amide proton T_1 1.5-fold of the average values used in these fits. [b] A ratio significantly under 1.0 indicates N-TIMP-1-induced exposure to higher hydrogen exchange rate. [c] A maximum rate of 1.4/s was assumed where an exchange peak is not observable. [d] A maximum rate of one per hour is assumed for this residue in free MMP-3(ΔC) on the basis of hydrogen−deuterium exchange measurements for the protease complexed with small synthetic inhibitors (*42*, *43*).

might be related to the modest N-TIMP-1-induced slowing of the amide proton exchange rates of Ile174 and Gly 173. The perturbation of the backbone of β strand V at residues 177 and 178 upon N-TIMP-1 binding occurs despite the low B factors of these sites in the X-ray structure of MMP-3(ΔC) inhibited by a small molecule (*41*).

Novel Active Site Hydrogen Bonding Inferred from Hydrogen Exchange Rates of Asn162 and Tyr223. The amide of Asn162 becoming protected from hydrogen exchange with water by at least eight-fold (and possibly orders of magnitude more; Table 1) suggests that it may form a hydrogen bond once N-TIMP-1 binds. We postulate that the amide of Asn162 of MMP-3(ΔC) forms a hydrogen bond with the carbonyl oxygen of Val4 of N-TIMP-1. The oxygen of Val4 is the closest potential hydrogen bond acceptor, about 4 Å from Asn162 N in X-ray models of the complex of MMP-3(ΔC) with TIMP-1 (W. Bode, personal communication). Surprisingly, N-TIMP-1 binding does not seem to protect Tyr223 of MMP-3(ΔC) from the paramagnetic probe (Figures 2B and 4). N-TIMP-1 binding, in fact, enhances the rate at which the Tyr223 amide exchanges with water more than 20-fold, to 28/s (Table 1 and Figure 2C). Thus the amide of Tyr223 lacks hydrogen bonding to N-TIMP-1 in solution. This contrasts the observation of a hydrogen bond between the amide of Tyr223 of MMP-3(ΔC) and the carbonyl oxygen of Cys3 of TIMP-1 in the crystallographic model of their complex (*40*). Similarly, Gooley and co-workers reported the absence of a hydrogen bond between the amide of Tyr223 of MMP-3(ΔC) and the backbone carbonyl of the P3′ residue of a small inhibitor, a hydrogen bond observed in the crystal structure of the identical complex (*42*). The amide of Tyr223 of MMP-3(ΔC) may lie at the edge of the interface with N-TIMP-1.

Considering both protection from paramagnetic solution probe and chemical shift perturbations, residues Tyr155, Asn162 through Ala169, Leu197 through Phe210, and Leu222 of MMP-3(ΔC) appear to be buried in the interface with N-TIMP-1, consistent with the crystallographic results of Bode and co-workers. Binding-linked exposure to the broadening agent can be readily identified as seen in the N-TIMP-1-induced exposure of backbone amides of Asp238, Asn240, Gly241, and Ser244 of helix C of MMP-3(ΔC). The exposure of helix C of MMP-3(ΔC) in solution agrees with the displacement of its N-terminus from helix C seen in the crystal structure of the complex with TIMP-1 (*40*). Thus, broadening of proton NMR lines by chelated gadolinium, comparing free protein with the protein bound to another protein, is a promising way to map the protein−protein interface in solution.

ACKNOWLEDGMENT

We thank Keith Brew and Yoshifuni Ito for helpful discussion.

SUPPORTING INFORMATION AVAILABLE

Figure 1 showing the normalized heights of the backbone amide NMR peaks of the uninhibited protease in the presence of 3 mM Gd−EDTA (top panel) and the normalized heights of the peaks of N-TIMP-1-inhibited MMP-3(ΔC) in the presence of 2 mM Gd−EDTA (bottom panel). Figure 2 showing fitted hydrogen exchange kinetics for four loop residues of MMP-3(ΔC) which experience a modest slowing in hydrogen exchange rate on the sub-second scale upon 1:1 binding of N-TIMP-1. Figure 3 showing changes in the protection or exposure of amides to hydrogen exchange (k_{free}/k_{bound}) in excess of 3-fold on a sub-second scale on the previously reported NMR model of MMP-3(ΔC) (4 pages).

REFERENCES

1. Nagase, H. (1996) in *Zinc metalloproteinases in health and disease*, pp 153-204, Taylor and Francis, London.
2. Matrisian, L. M. (1992) *BioEssays 14*, 455-463.
3. Birkedal-Hansen, H., Moore, W. G. I., Bodden, M. K., Windsor, L. J., Birkedal-Hansen, B., DeCarlo, A., and Engler, J. A. (1993) *Crit. Rev. Oral Biol. Med. 4*, 197−250.
4. Woessner, J. F., Jr. (1991) *FASEB J. 5*, 2145−2154.
5. Murphy, G., and Willenbrock, F. (1995) *Methods Enzymol. 248*, 496−510.
6. Murphy, G., Houbrechts, A., Cockett, M. I., Williamson, R. A., O'Shea, M., and Docherty, A. J. P. (1991) *Biochemistry 30*, 8097−8102.
7. Williamson, R. A., Bartels, H., Murphy, G., and Freedman, R. B. (1994) *Protein Eng. 7*, 1035−1040.

8. Huang, W., Suzuki, K., Nagase, H., Arumugam, S., Van Doren, S. R., and Brew, K. (1996) *FEBS Lett. 384*, 155−161.
9. Williamson, R. A., Martorell, G., Carr, M. D., Murphy, G., Docherty, A. J. P., Freedman, R. B., and Feeney, J. (1994) *Biochemistry 33*, 11745−11759.
10. Williamson, R. A., Carr, M. D., Frenkiel, T. A., Feeney, J., and Freedman, R. B. (1997) *Biochemistry 36*, 13882−13889.
11. Chen, Y., Reizer, J., Saier, M. H. J., Fairbrother, W. J., and Wright, P. E. (1993) *Biochemistry 32*, 32−37.
12. Gronenborn, A. M., and Clore, G. M. (1993) *J. Mol. Biol. 233*, 331−335.
13. Paterson, Y., Englander, S. W., and Roder, H. (1990) *Science 249*, 755−759.
14. Petros, M. A., Mueller, L., and Kopple, D. K. (1990) *Biochemistry 29*, 10041−10048.
15. Esposito, G., Lesk, M. A., Molinari, H., Motta, A., Niccolai, N., and Pastore, A. (1992) *J. Mol. Biol. 224*, 659−670.
16. Fesik, S. W., Gemmecker, G., Olejniczak, E. T., and Petros, A. M. (1991) *J. Am. Chem. Soc. 113*, 7080−7081.
17. Muchmore, D. C., McIntosh, L. P., Russell, C. B., Anderson, D. E., and Dahlquist, F. W. (1989) *Methods Enzymol. 177*, 44−73.
18. Hibler, D. W., Harpold, L., Dell'Acqua, M., Pourmatabbed, T., Gerlt, J. A., Wilde, J. A., and Bolton, P. H. (1989) *Methods Enzymol. 177*, 74−86.
19. Suzuki, K., Kan, C.-C., Huang, W., Gehring, M. R., Brew, K., and Nagase, H. (1998) *Biological Chemistry Hoppe−Seyler 379*, 185−191.
20. Marcy, A. I., Eiberger, L. L., Harrison, R., Chan, H. K., Hutchinson, N. I., Hagmann, W. K., Cameron, P. M., Boulton, D. A., and Hermes, J. D. (1991) *Biochemistry 30*, 6476−6483.
21. Knight, C. G., Willenbrock, F., and Murphy, G. (1992) *FEBS Lett. 296*, 263−266.
22. Van Doren, S. R., Kurochkin, A. V., Ye, Q. Z., Johnson, L. L., Hupe, D. L., and Zuiderweg, E. R. P. (1993) *Biochemistry 32*, 13109−13122.
23. Mori, S., Abeygunawardana, C., O'Neil Johnson, M., and Van Zijl, C. M. P. (1995) *J. Magn. Reson., Ser. B 108*, 94−98.
24. Shaka, A. J., Barker, P. B., and Freeman, R. (1985) *J. Magn. Reson. 64*, 547−552.
25. Marion, D., Ikura, M., Tschudin, R., and Bax, A. (1989) *J. Magn. Reson. 85*, 393−399.
26. Grzesiek, S., and Bax, A. (1992) *J. Magn. Reson. 96*, 432−440.
27. Boucher, W., Laue, E. D., Campbell-Burk, S., and Domaille, P. J. (1992) *J. Am. Chem. Soc. 114*, 2262−2264.
28. Boucher, W., Laue, E. D., Campbell-Burk, S. L., and Domaille, P. J. (1993) *J. Biomol. NMR 2*, 631−637.
29. Bax, A., and Pochapsky, S. S. (1992) *J. Magn. Reson. 99*, 638−643.
30. Sklenar, V., Piotto, M., Leppik, R., and Saudek, V. (1993) *J. Magn. Reson., Ser. A 102*, 241−245.
31. Zhu, G., and Bax, A. (1990) *J. Magn. Reson. 90*, 405−410.
32. Fesik, S. W., and Zuiderweg, E. R. P. (1988) *J. Magn. Reson. 78*, 588−593.
33. Farmer, B. T., Constantine, K. L., Goldfarb, V., Friedrichs, M. F., Wittekind, M., Yanchunas, J. J., Robertson, J. G., and Mueller, L. (1996) *Nat. Struct. Biol. 3*, 995−997.
34. Kemple, K. D., Ray, B. D., Lipkowitz, K. B., Prendergas, F. G., and Rao, B. D. N. (1988) *J. Am. Chem. Soc. 110*, 8275−8287.
35. Mori, S., Berg, M. J., and Van Zijl, C. M. P. (1996) *J. Biomol. NMR 7*, 77−82.
36. Dayie, T. K., and Wagner, G. (1994) *J. Magn. Reson., Ser. A 111*, 121−126.
37. Geen, H., and Freeman, R. (1991) *J. Magn. Reson. 93*, 93−141.
38. Mori, S., Abeygunawardana, C., van Zijl, P. C. M., and Berg, J. M. (1996) *J. Magn. Reson. Ser. B 110*, 96−101.
39. Jeener, J., Meier, B. H., Bachmann, P., and Ernst, R. R. (1979) *J. Chem. Phys. 71*, 4546−4553.
40. Gomis-Ruth, F.-X., Maskos, K., Betz, M., Bergner, A., Huber, R., Suzuki, K., Yoshida, N., Nagase, H., Brew, K., Bourenkov, G. P., Bartunik, H., and Bode, W. (1997) *Nature 389*, 77−81.
41. Becker, J. W., Marcy, A. I., Rokosz, L. L., Axel, M. G., Burbaum, J. J., Fitzgerald, P. M. D., Cameron, P. M., Esser, C. K., Hagmann, W. K., Hermes, J. D., and Springer, J. P. (1995) *Protein Sci. 4*, 1966−1976.
42. Gooley, P. R., Johnson, B. A., Marcy, A. I., Cuca, G. C., Axel, M. G., Caldwell, C. G., Hagmann, W. K., and Becker, J. W. (1996) *J. Biomol. NMR 7*, 8−28.
43. Van Doren, S. R., Kurochkin, A. V., Hu, W. D., Ye, Q. Z., Johnson, L. L., Hupe, D. L., and Zuiderweg, E. R. P. (1995) *Protein Sci. 4*, 2487−2498.
44. Koradi, R., Billeter, M., and Wuthrich, K. (1996) *J. Mol. Graphics 14*, 51−55.

BI980128H